Article

Characterisation of Macrophage Inhibitory Factor-2 (MIF-2) in *Haemonchus contortus* and *Teladorsagia circumcincta*

Saleh Umair [1,*], **Jacqueline S. Knight** [1], **Charlotte Bouchet** [1], **Nikola Palevich** [1], **Sheralee B. Cleland** [1], **Warwick Grant** [2] **and Heather V. Simpson** [3]

1   AgResearch Ltd., Hopkirk Research Institute, Grasslands Research Centre, Tennent Drive, Private Bag 11-008, Palmerston North 4442, New Zealand
2   Department of Physiology Anatomy and Microbiology, School of Life Sciences, La Trobe University, Bundoora 3083, Australia
3   Institute of Veterinary, Animal and Biomedical Sciences, Massey University, Private Bag 11-222, Palmerston North 4442, New Zealand
*   Correspondence: saleh.umair@agresearch.co.nz

Abstract: Full-length cDNAs encoding macrophage inhibitory factor-2 (MIF-2) were cloned from *Teladorsagia circumcincta* (*Tc*MIF-2) and *Haemonchus contortus* (*Hc*MIF-2). *Tc*MIF-2 and *Hc*MIF-2 cDNA (342 bp) encoded proteins of 114 amino acids, each of which was present as a single band of about 16 kDa on SDS-PAGE. Multiple alignments of the protein sequences showed homology of 84% between *Tc*MIF-2 and *Hc*MIF-2, 54–76% with MIF-2s of seven nematodes, but low homology with other MIF sequences. The predicted three-dimensional structures revealed an overall structural homology of *Tc*MIF-2 and *Hc*MIF-2, highly conserved binding and catalytic sites and minor differences in the tautomerase binding site residues in other nematode MIF-2 homologues. A phylogenetic tree was constructed using helminth and mammalian MIF-1 and MIF-2 sequences. Soluble C-terminal MIF-2 proteins were cloned in arabinose inducible promotor AY2.4, expressed in *Escherichia coli* strain AY2.4 and purified. Recombinant *Tc*MIF-2 and *Hc*MIF-2 had similar enzyme activities in a standard tautomerase assay. Recombinant *Hc*MIF-2 activity was approximately halved by storage at 4 °C, −20 °C or −70 °C. Antibodies in serum and saliva from field-immune, but not nematode-naïve, sheep recognised recombinant *Hc*MIF-2 and *Tc*MIF-2 in enzyme-linked immunosorbent assays. Recognition of the recombinant proteins by antibodies generated by exposure of sheep to the native enzyme indicates similar antigenicity of the two proteins.

Keywords: cloning; expression; ELISA; *Teladorsagia circumcincta*; *Haemonchus contortus*; kinetic properties; macrophage inhibitory factor-2; MIF-2

1. Introduction

The abomasal nematode parasites *Haemonchus contortus* and *Teladorsagia circumcincta* cause significant loss of production and ill-health in sheep and goats. Widespread resistance to anthelmintics has necessitated developing alternative parasite control strategies, such as vaccination, which involves identification of antigens or combinations of antigens, appropriate adjuvants and vaccination protocols. Amongst the most promising antigens are multifunctional proteins, which allow the host immune response to disrupt worm physiology at more than point.

Macrophage migration inhibitory factors (MIFs), theta class glutathione transferases (GSTs) with oxido-reductase and tautomerase activities [1], are ligands of the CD74 cell receptor [2]. MIF was originally identified as a T-cell pro-inflammatory cytokine [3,4], but has subsequently been shown to be expressed in other tissues, where it has tissue-specific actions and generally promotes cell survival and inhibits senescence [5]. In humans, MIF antagonises the effects of aging and ameliorates age-related diseases [6,7]. Many of these properties are shared with non-mammalian MIF proteins [8], including those in

free-living and parasitic nematodes [9–16], although some biochemical differences were apparent between nematode and mammalian MIF proteins in substrate affinity [17] and sensitivity to inhibitors [12] of the tautomerase activity. Importantly, MIF proteins released by parasitic nematodes were able to modify the host immune response and promote parasite survival [16,18–20].

In contrast to the single *mif* gene in mammals, gene duplication in nematode lineages has resulted in multiple genes. There are four *mif* genes in *Caenorhabditis elegans* [21], encoding proteins which are 15–30% identical to each other. MIF-1 and MIF-2 proteins have been identified in parasitic nematodes, with MIF-1 being more similar to mammalian MIF [9]. *H. contortus* MIF-1 and MIF-2 are both involved in larval development; RNAi using either *mif-1* or *mif-2* dsRNA resulted in strong developmental delay phenotypes: the majority after *mif-1* knockout were arrested/killed at L1 and only 23% reached the L3 stage, whereas for MIF-2, 59% of worms became L3 and the others were mainly arrested at the L2 stage (unpublished data). In contrast, *mif-1* knockout in *C. elegans* does not confer an obvious deleterious phenotype, whereas both *mif-2* RNAi and a deletion mutant are embryonic lethal [21]. Interestingly, Nisbet et al. [11] did not find either their recombinant or purified native *Tc*MIF-1 influenced sheep monocyte migration. These inconsistent observations suggest that both MIF-1 and MIF-2 could be candidate vaccine antigens and that the superiority of either one in a multi-antigen vaccine against abomasal nematodes remains to be assessed.

In the present study, cDNAs encoding *T. circumcincta* (*Tc*MIF-2) and *H. contortus* MIF-2 (*Hc*MIF-2) were cloned, expressed in *Escherichia coli* and the recombinant proteins purified. Tautomerase activity of both recombinant enzymes was confirmed. Enzyme-linked immunosorbent assays (ELISAs) were performed to determine if the recombinant proteins were recognised by antibodies in saliva and serum from immune sheep previously exposed to a wide range nematode parasites in the field.

2. Materials and Methods

All chemicals were purchased from the Sigma Chemical Co. (St. Louis, MO, USA) unless stated otherwise.

2.1. Parasites

Pure cultures of *T. circumcincta* and *H. contortus* were maintained in the laboratory by regular passage through sheep. Adult worms were recovered from the abomasa of infected sheep, as described previously [22]. Briefly, abomasal contents were mixed 2:1 with 3% agar and the solidified agar blocks incubated at 37 °C in a saline bath. Clumps of parasites were collected from the saline soon after emergence and frozen in Microcentrifuge tubes (Salt Lake City, UT, USA) at −80 °C for molecular biology procedures.

2.2. RNA Isolation and Synthesis of cDNA

Adult *T. circumcincta* or *H. contortus* (50–100 µL packed volume) in 1 mL Trizol (Life Technologies, Carlsbad, CA, USA) were ground to a fine powder in a mortar under liquid N$_2$ and RNA was extracted according to the manufacturer's instructions. The quality and concentration of the RNA was assessed, and first strand cDNA synthesised from 1 µg using the iScript Select cDNA Synthesis Kit (Bio-Rad, Auckland, New Zealand) and a 1:1 mixture of Oligo (dT)$_{20}$ and random primers.

The full-length *H. contortus* MIF-2 sequence was amplified from cDNA in a PCR containing the oligonucleotide primers *Hcmif*-2FLF (5′-CCTATGGTAAGAGTTGC-3′) and *Hcmif*-2FLR (5′-CGACAGTTGCAGCTGCCAC-3′). These primers were developed from the publically available *H. contortus* MIF-2 EST sequence (HC07649). Initially, the primers *Hcmif*-2 FLF and *Hcmif*-2 FLR were designed and used to amplify the *H. contortus* MIF-2 coding region from *H. contortus* adult cDNA using the Expand High Fidelity PCR system according to the manufacturer's instructions (ThermoFisher Scientific, Waltham, USA). The resulting amplification product was cloned into pCR4-TOPO using the TOPO TA

cloning kit for sequencing (ThermoFisher Scientific, Waltham, USA) and sequenced to confirm identity. The restriction enzyme sites NdeI and NotI were added to the *H. contortus* MIF-2 coding region using the oligonucleotide primers *Hcmif*-2-NdeIF and *Hcmif*-2-NotIR, the pCR4 clone as template and the Expand High Fidelity PCR system. The product was digested with NdeI and NotI before cloning into the similarly digested expression vector AY2.4 [23] to generate a construct which enabled the arabinose-inducible production of a recombinant C-terminal His- and E-tagged *H. contortus* MIF-2 fusion protein in *E. coli*.

A partial *T. circumcincta* MIF-2 sequence TDC15440 (AgResearch's Internal database), 3′ RACE primers (*Tcmif*F-2_RACE-F1 (5′-CACTGACATATTGGCGGAGTCCATG-3′) and *Tcmif*-2_RACE-F2 (5′-GTTTACGCTGGCCAGCGCATTATG-3′) were used to obtain the 3′ of the gene. Subsequently, the full-length *T. circumcincta* MIF-2 sequence was amplified from cDNA in a PCR containing the oligonucleotide primers *Tcmif*-2-NdeIF (5′-ATCGCATATGCCGATGGTGAGAGTTGC-3′) and *Tcmif*-2-NotIR (5′-GATCGCGGCCGCG ACGGTTGCAGCGGCCAC-3′). The full-length gene was cloned, using standard protocols, into the expression vector AY2.4 using the restriction enzymes Ndel and Notl (engineered into the forward and reverse primers, underlined in primer sequences) to allow the production of C-terminal His-tagged recombinant protein. The expression clone was sequenced to confirm identity.

The Muscle alignment option in Geneious Prime (Biomatters Ltd., Auckland, New Zealand) with the Blosum 62 similarity matrix was used to determine 100% similarity of *Tc*MIF-2 to *H. contortus* and other MIFs. The active and binding sites labelled were identified in the structural modelling (see Section 2.3). A phylogenetic tree of *Tc*MIF-2 and *Hc*MIF-2 and their helminth homologues was constructed, using the genetic distance model of Jukes-Canter by the neighbour joining method in Geneious Prime (Auckland, New Zealand).

2.3. Protein Modelling and Structural Analysis of TcMIF-2 and HcMIF-2

The Position-Specific Iterative Basic Local Alignment Search Tool (PSI-BLAST) [24] was used to compare the *Tc*MIF-2 and HcMIF-2 protein sequences with deposited structures in the Protein Data Bank (PDB). The structural models of *Tc*MIF-2 and *Hc*MIF-2 were constructed by submitting the amino acid sequences obtained to the I-TASSER server [25]. For *Tc*MIF-2, only one model was obtained, and for *Hc*MIF-2 a model was selected from the best of five possible models generated. The structural model with highest C-score was further validated using Procheck [26] and ProSA-web [27]. The substrate binding domains were identified, and active site residues deduced using PyMol [28].

2.4. Expression of Recombinant TcMIF-2 and HcMIF-2 in E. coli

E. coli strain BL21 (DE3) transformed with *E. coli Tc*MIF-2 or *Hc*MIF-2 in AY2.4 to allow the production of N-terminal His tagged recombinant proteins under the control of the heat-inducible tandem λP_R and P_L promoters [29]. The culture was grown in 10 mL Luria Broth (LB) supplemented with 100 µg/mL ampicillin for 16 h at 37 °C and 250 rpm. The culture was diluted 20-fold in LB with 100 µg/mL ampicillin and grown to OD_{600nm} of 0.6–0.8 at 37 °C and 250 rpm. L-arabinose was added to a final concentration of 0.2% and the culture grown for an additional 4 h at 30 °C and 250 rpm. The pellet was weighted and resuspended in 10 mL per gram of pelleted bacteria of equilibration buffer (20 mM sodium bi-phosphate, 0.5 M NaCl, 20 mM Imidazole, pH 7.4). Protease inhibitors were added to the suspension, which was then passed through, the chamber of a MP110 Microfluidizer® (Microfluidics, Westwood, CA, USA) seven times consecutively under ice, at 20,000 psi to ensure the complete lysis of *E. coli* as recommended by the manufacturer. The crude lysate was centrifuged at 15,000× *g* for 20 min at 4 °C to remove all cell debris, and the supernatant was collected and filtered through a 0.22 µm filter.

2.5. Purification

Purified recombinant poly-histidine protein was obtained by Fast Protein Liquid Chromatography (FPLC) under native conditions using a HispTap HP column (GE Healthcare, Chicago, IL, USA), and the BioLogic DuoFlow chromatography system (Bio-Rad, Auckland, New Zealand). Sodium biphosphate buffer was used as an equilibration buffer, sodium biphosphate containing 20 mM imidazole as the wash buffer and sodium biphosphate containing 500 mM imidazole as elution buffer. Following the elution, the protein was dialysed overnight, and the concentration was determined by the Nanodrop 1000[TM] (Thermo Scientific, Waltham, MA, USA) using the A280 nm assay using the extinction coefficient 4470 $M^{-1}cm^{-1}$ and the molecular weight 16 KDa.

2.6. Gel Electrophoresis

SDS-PAGE was performed using NuPAGE Novex 4–12% Bis-Tris gels according to the instructions of the manufacturer (Invitrogen, Waltham, MA, USA). Gels were stained with SimplyBlue[TM] SafeStain (Invitrogen Waltham, MA, USA). A Western blot was also performed on the protein using a monoclonal anti-polyhistidine-peroxidase antibody. Blots were incubated overnight in 1:2000 antibody in buffer (4% skim milk powder in Tris-buffered saline and 0.1% Tween-20) at room temperature and developed to detect His-tagged recombinant protein.

2.7. HcMIF-2 and TcMIF-2 Assays

The tautomerase activities of recombinant *Hc*MIF-2 and *Tc*MIF-2 were determined from the tautomerisation of the coloured dopachrome methyl ester to its colourless enol form [30]. Dopochrome methyl ester was prepared by mixing 4 mM L-3,4-dihydroxylphenylalanine methyl ester with 8 mM sodium periodate in potassium phosphate buffer (25 mM potassium phosphate pH 6.0, 0.5 mM EDTA) for 5 min at room temperature before placing on ice for 20 min. The decrease in absorbance at 475 nm was monitored at room temperature over a 5 min period in a cuvette (1 mL final volume) containing 20 µg recombinant enzyme in assay buffer containing dopochrome methyl ester (final OD_{475nm} 0.7–0.9). Background readings were taken before the addition of recombinant enzyme.

The effect on tautomerase activity of varying the concentration of recombinant *Hc*MIF-2 in the assay from 2–20 µg/mL of protein was determined. The effect of storage of recombinant *Hc*MIF-2 at 4 °C, −20 °C and −70 °C for 16 h on enzyme activity was determined and the activities of two separate batches of FPLC-purified recombinant *Hc*MIF-2 were compared.

2.8. ELISA

Pooled serum and saliva samples collected from parasite-naive and parasite-exposed sheep were tested by ELISA for the presence of antibodies that react with recombinant *Tc*MIF-2 or *Hc*MIF-2. Serum and saliva samples were collected from 18 male 6–7 months-old Romney lambs previously exposed to multiple species of parasite, including *H. contortus* and *T. circumcincta*. These lambs had developed immunity against *T. circumcincta* infection. 5 µg/mL *Tc*MIF-2 or *Hc*MIF-2 were immobilised onto ELISA plates (Maxisorp, Thermo Scientific), free binding sites were blocked with Superblock (Thermo Scientific), followed by incubation for 2 h at room temperature with serial dilutions of serum (200- to 6400-fold) or saliva (20- to 160-fold) in ELISA buffer. Bound serum immunoglobulins were then detected by incubation for 2 h at 37 °C with 1:4000 diluted rabbit anti-sheep IgG-HRP and colour development with 3,3′,5,5′-tetramethylbenzidine (TMB). Salivary IgA was similarly detected with rabbit anti-sheep IgA-HRP.

3. Results

3.1. TcMIF-2 and HcMIF-2 Gene Sequences

The 342 bp full-length *T. circumcincta* and *H. contortus* cDNA sequences, amplified from adult *T. circumcincta* and *H. contortus* cDNA, respectively, have been deposited in Genbank. The predicted proteins consisted of 114 amino acids (Figure 1).

```
                                            1                                                          60
                                            |  **                                   **  *             |
                           TcMIF-2          MPMVRVATNIP-DKDVPPNFEERLTDILAESMNKPRTRIAVEVYAGQRIMHGGVRN--P
                           HcMIF-2          MPMGRVATNLP-DKDVPANFEERLTDLLAESMNKPRARIAVEMMAGQRIMHGGVRN--P
       Heligmosomoides polygyrus MIF-2      MPMVSVATNIP-DKDVPANFEERLTDVLAESMSKPRSRIAIEVFAGARILHGGVRN--P
              Ancylostoma caninum MIF-2      MPPVRVATNLP-DKDVPANFEERLTDILADSMNKPRNRIAIEVMAGQRITHGASRN--P
    Parastrongyloides trichosuri MIF-2      --------NLQ-NEKVPEDFFPKLTELLAESMGKPVNRIAAELSPSARLIHGGSKD--P
          Caenorhabditis elegans MIF-2      -----------------------MGGKPRERIAVEIAAGARLVHGATHD--P
         Caenorhabditis briggsae MIF-2      MPMVRVATNLP-DEKVPQDFEIRLTDLLARSMGKPRERIAVEVAAGARLVHGATHD--P
                     Brugia malayi MIF-2      MPLITLASNVP-ASRFPSDFNVQFTELMAKMLGKPTSRILLLVMPNAQLSHGTTEN--P
               Onchocerca volvulus MIF-2      MPLITLASNVL-ASGFPTDFSVQFTKLMAELLGKPISRITLLVTPSAQLSRGATQD--P
        Oesophagostomum dentatum MIF-2      MPMVRVATNLP-DKDVPANFEERLTDLLSESMNKPKSRIAVEIYAGQRIIHGASRS--P
            Ancylostoma ceylanicum MIF-2      MPMVRVATNLP-DKDVPANFEERLTDLLAESMNKPRNRIAIEVLAGQRITHGASRN--P
                      Ascaris suum MIF-2      MPLVTLASNVA-DEKFPVDFNQQFTNFLSNLIEKPAARISLLVMTGARLTHGGSND--P
          Caenorhabditis elegans MIF-1      MPVFSINVNVKVPAEKQNEILKELSTVLGKLLNKPEQYMCIHFHEDQGILYAGTTE--P
          Caenorhabditis elegans MIF-3      MPVIKVQTNV---KKVSDGFEVRLAIHMAKVMKRPESQIFVSLDMNSRMTRGQLTD--P
          Caenorhabditis elegans MIF-4      MQVVRIQTNIR-SADIPEKFEQDVIYNLSVVMELPADKFVIIVEPAVRMRIGFENKEIP
                       Mus musculus MIF      MPMFIVNTNVP-RASVPEGFLSELTQQLAQATGKPAQYIAVHVVPDQLMTFSGTND--P
                      Gallus gallus MIF      MPMFTIHTNVC-KDAVPDSLLGELTQQLAKATGKPAQYIAVHIVPDQMMSFGGSTD--P
                          Ovis aries MIF      MPMFVVNTNVP-RASVPDGLLSELTQQLAQATGKPAQYIAVHVVPDQLMTFGGSSE--P
                         Bos taurus MIF      -PMFVVNTNVP-RASVPDGLLSELTQQLAQATGKPPQYIAV------------------
                       Homo sapiens MIF      MPMFIVNTNVP-RASVPDGFLSELTQQLAQATGKPPQYIAVHVVPDQLMAFGGSSE--P
```

```
                                            61                                                        120
                                            |  ***                                        *      *   *|
                           TcMIF-2          VVIIKIESIGAL-EPDKNIRHTERVTQLCQDVLHVPKDKVVISYFDLAPTNVGFGGTTVA
                           HcMIF-2          VVLIKVESIGAL-DPDSTIRHTQKVTQLCTEVLHVPKDKVTISYFDLAPTNVSFAGTTVA
       Heligmosomoides polygyrus MIF-2      VAIIKIESIGSM-TPEDNIRHTQKVTQLCQQALNLPKEKVVISFFDLSPTNVGFGGTTVA
              Ancylostoma caninum MIF-2      VAVIKVESIGAL-SADDNIRHTQKITQFCQDTLKLPKDKVIITYFDLQPIHVGFNGTTVA
    Parastrongyloides trichosuri MIF-2      VVVITIKSIGAL-SPSDNIRHTEKVTALCREKLGLPLDKVVIDFVNLSPNDVGFAGTTVA
          Caenorhabditis elegans MIF-2      VTVISIKSIGAV-SAEDNIRNTAAITEFCGKELGLPKDKVVITFHDLPPATVGFNGTTVA
         Caenorhabditis briggsae MIF-2      ATVISIKSIGAV-SAEDNIRHTAAITEFCGKELGLPKDKVVITFHDMAPVTVGFNGTTVA
                     Brugia malayi MIF-2      SCFTVVKSIGSF-SADKNIEYSSLISEFMKKTLDIDPAHCIIHFLNLDPENVGCNGTTMK
               Onchocerca volvulus MIF-2      TCLIVIKSIGSF-SADKNIKYSGSISEFIKKTLNIDPAYCIIHFLDLNPEDIGCNGTTMK
        Oesophagostomum dentatum MIF-2      VVLIKIEAIGSM-SAEDNIRHTQKITQLCQDALKLPKDK--------------------
            Ancylostoma ceylanicum MIF-2      VAVIKVESIGAL-SADDNIRHTQKITQFCQDTLKLPKDKVIITYFDLQPIHVGFNGTTVA
                      Ascaris suum MIF-2      TCVITVKAIGAF-NDELNVKYSAKIAEFIHQSLAIAPEKCLIEFVNLEPQNVSNSGTTMK
          Caenorhabditis elegans MIF-1      AGFAVLKSIGGVGSAKQNNAISAVVFPIIEKHLGIPGNRLYIEFVNLGAADIAYNGQTFA
          Caenorhabditis elegans MIF-3      LAVLDVTSSTVL-TPILTEEYTVALCEFFSQELALDSDAVLINYRSLSPELIGFNGHILT
          Caenorhabditis elegans MIF-4      VAIVNFQTTRPS-SRIENDSYAKKLTSVLNEQLKLDPAHIFISFDFKDAKSFATQGKTIA
                       Mus musculus MIF      CALCSLHSIGKI-GGAQNRNYSKLLCGLLSDRLHISPDRVYINYYDMNAANVGWNGSTFA
                      Gallus gallus MIF      CALCSLYSIGKI-GGQQNKTYTKLLCDMIAKHLHVSADRVYINYFDINAANVGWNGSTFA
                          Ovis aries MIF      CALCSLHSIGKI-GGAQNRSYSKLLCGLLTERLRISPDRIYINFCDMNAANVGWNGSTFA
                         Bos taurus MIF      ----------------------------------------------------------
                       Homo sapiens MIF      CALCSLHSIGRI-GGAQNRSYSKQLCGLLAERLRISPDRVYINYYDMNAANVGWNNSTFA
```

```
                                            121
                                            |
                                                                                % identity
                           TcMIF-2          AATVAAAGAPVPYPDPLE---------------
                           HcMIF-2          AATV----------------------------         [84%]
       Heligmosomoides polygyrus MIF-2      AATV----------------------------         [80%]
              Ancylostoma caninum MIF-2      AATM----------------------------         [75%]
    Parastrongyloides trichosuri MIF-2      AANK----------------------------         [55%]
          Caenorhabditis elegans MIF-2      EANKK---------------------------         [54%]
         Caenorhabditis briggsae MIF-2      ETNKL---------------------------         [59%]
                     Brugia malayi MIF-2      ELMKK---------------------------         [29%]
               Onchocerca volvulus MIF-2      ELMKK---------------------------         [29%]
        Oesophagostomum dentatum MIF-2      --------------------------------         [73%]
            Ancylostoma ceylanicum MIF-2      AATM----------------------------         [76%]
                      Ascaris suum MIF-2      VLMSKK--------------------------         [30%]
          Caenorhabditis elegans MIF-1      --------------------------------         [21%]
          Caenorhabditis elegans MIF-3      ENRPFISTDRARFIIGVLGIAFLAFLLQFLKYI        [28%]
          Caenorhabditis elegans MIF-4      SLYE----------------------------         [22%]
                       Mus musculus MIF      --------------------------------         [37%]
                      Gallus gallus MIF      --------------------------------         [35%]
                          Ovis aries MIF      --------------------------------         [33%]
                         Bos taurus MIF      --------------------------------         [44%]
                       Homo sapiens MIF      --------------------------------         [35%]
```

Figure 1. Multiple protein sequence alignment of *T. circumcincta* MIF-2, *H. contortus* MIF-2, *Heligmosomoides polygyrus* MIF-2 (GI: VDO97074), *Ancylostoma caninum* MIF-2 (GI: ABU68338), *Parastrongyloides trichosuri* MIF-2 (GI: BM513256), *Caenorhabditis elegans* MIF-2 (GI: NP_001256387.1), *Caenorhabditis briggsae* MIF-2 (GI: CAP39673.2), *Brugia malayi* MIF-2 (GI: AAF91074), *Onchocerca volvulus* MIF-2 (GI: AAK66564), *Oesophagostomum dentatum* MIF-2 (GI: KHJ75996.1), *Ancylostoma ceylanicum* MIF-2 (GI: ABO31935), *Ascaris suum* MIF-2 (GI: ADY48840), *Caenorhabditis elegans* MIF-1 (GI: NP_499536.1), *Caenorhabditis elegans* MIF-3 (GI: NP_492069), *Caenorhabditis elegans* MIF-4 (GI: NP_500968.1), *Mus musculus* MIF (GI: P34884-1), *Gallus gallus* MIF (GI: NP_001292020), *Ovis aries* MIF (GI: NP_001072123), *Bos tautus* MIF (GI: NP_001028780) and *Homo sapiens* MIF (GI: CAG46452). *Tc*MIF-2 and *Hc*MIF-2 catalytic and active residues are marked by an asterisk (*). The % homology of each sequence with *Teci*MIF-2 is shown at the end of the alignment.

Multiple alignments of the protein sequences of *Tc*MIF-2 and *Hc*MIF-2 with homologues from *Heligmosomoides polygyrus*, *Ancylostoma caninum*, *Parastrongyloides trichosuri*,

C. elegans, *Caenorhabditis briggsae*, *Brugia malayi*, *Onchocerca volvulus*, *Oesophagostomum den-tatum*, *Ancylostoma ceylanicum* and *Ascaris suum*, and MIFs from *C. elegans*, *Mus musculus*, *Gallus gallus*, *Ovis aries*, *Bos taurus* and *Homo sapiens*, are shown in Figure 1. Residues involved in tautomerase activity in *Tc*MIF-2 and *Hc*MIF-2, marked by an asterisk, were largely conserved in the MIF-2s of several nematode species. There was 84% homology between *Tc*MIF-2 and *Hc*MIF-2 and 54–76% homology between MIF-2s of seven nematodes, but there was low homology with the other MIF sequences in the multiple alignment.

A search using PSI-BLAST against the Protein Data Bank (PDB) showed that the amino-acid sequences of *Tc*MIF-2 and *Hc*MIF-2 resulted in the assignment of a putative function to two of the top blast hits annotated as hypothetical protein (locus tag EYC32381 to EYC32384 of *A. ceylanicum*) and protein of unknown function (locus tag VDO97074 of *H. polygyrus*) with 65–75% and 80% identity, respectively.

In another alignment, the amino acid sequence of *Hc*MIF-2 corresponded to the product of the gene designated as HCON_NP_LOC13552 located on chromosome 5 (Gen-Bank accession number CP035803, BioProject accession number PRJNA517503) from the *H. contortus* NZ_Hco_NP genome version 1.0 [31].

The phylogenetic tree using multiple helminth and mammalian MIF sequences (Figure 2) revealed that the *Tc*MIF-2 was most closely related to the MIF-2 of the nematode *H. contortus* and less like other MIFs (MIF-1, MIF-3, MIF-4) from helminths and mammals. The phylogenetic tree also revealed that MIF-1 and MIF-2 are two distinct families and clearly separated from each other.
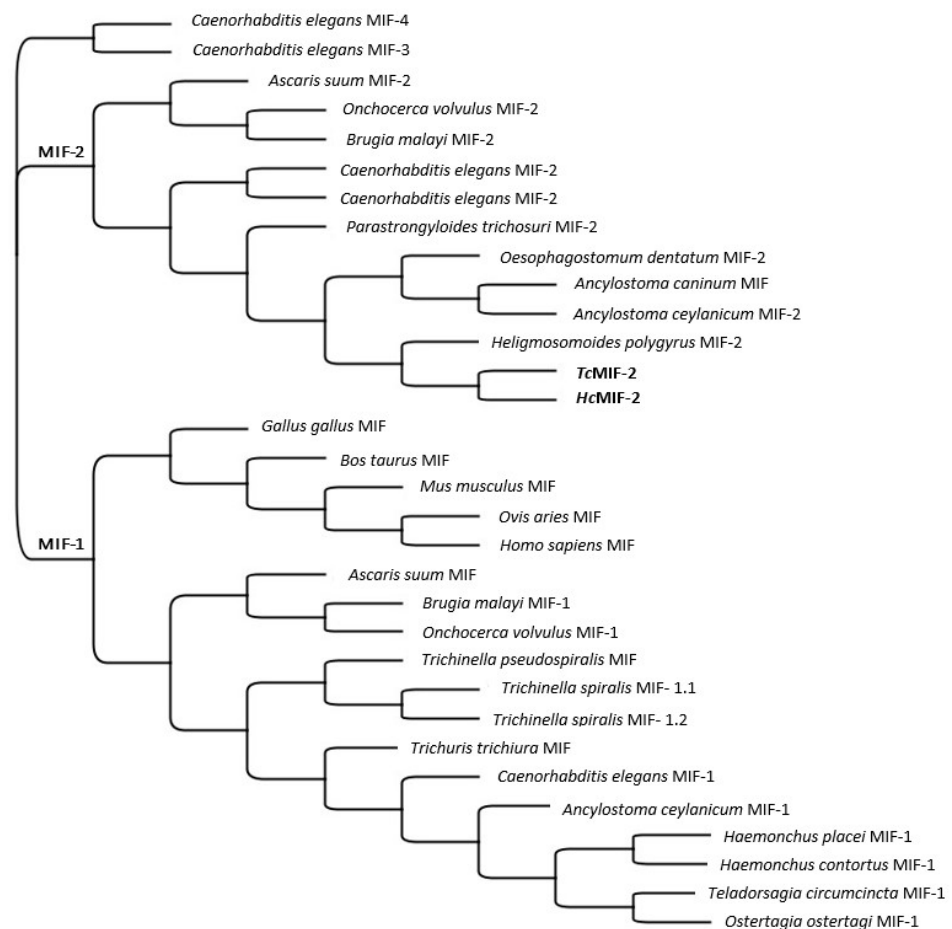

Figure 2. Phylogenetic tree of *T. circumcincta* MIF-2, *H. contortus* MIF-2, *Caenorhabditis elegans* MIF-2 (GI: NP_001256387.1), *Caenorhabditis elegans* MIF-3 (GI: NP_492069), *Caenorhabditis elegans* MIF-4 (GI:

NP_500968.1), *Caenorhabditis briggsae* MIF-2 (GI: CAP39673.2), *Heligmosomoides polygyrus* MIF-2 (GI: VDO97074), *Parastrongyloides trichosuri* MIF-2 (GI: BM513256), *Ancylostoma ceylanicum* MIF-2 (GI: ABO31935), *Onchocerca volvulus* MIF-2 (GI: AAK66564), *Brugia malayi* MIF-2 (GI: AAF91074), *Ancylostoma caninum* MIF (GI: ABU68338), *Ascaris suum* MIF-2 (GI: ADY48840), *Oesophagostomum dentatum* MIF-2 (GI: KHJ75996.1), *Mus musculus* MIF (GI: P34884-1), *Gallus gallus* MIF (GI: NP_001292020), *Ovis aries* MIF (GI: NP_001072123) *Homo sapiens* MIF (GI: CAG46452), *Ostertagia ostertagi* MIF-1 (GI: AIE56464.1), *T. circumcincta* MIF-1 (GI: PIO59269.1), *H. contortus* MIF-1, *Haemonchus placei* MIF-1 (GI: VDO39061.1), *A. ceylanicum* MIF-1 (GI: ACC54555.1), *Caenorhabditis elegans* MIF-1 (GI: NP_499536.1), *Trichuris trichiura* MIF (GI: CAB46355), *Trichinella spiralis* MIF-1.1 (GI: XP_003378412.1), *Trichinella spiralis* MIF-1.2 (GI: CAB46354), *Trichinella pseudospiralis* MIF (GI: AAL12630), *O. volvulus* MIF-1 (GI: AAK66563), *B. malayi* MIF-1 (GI: U88035.1) and *A. suum* MIF-1 (GI: BAD24819) using the genetic distance model of Jukes-Canter by the neighbour joining method in Geneious Prime.

3.2. MIF-2 Structure

The predicted 3D structures of *Tc*MIF-2 and *Hc*MIF-2 and binding and catalytic sites over a wide range of ligands are shown in Figure 3. The protein structures of both *Tc*MIF-2 and *Hc*MIF-2 best fit superimposed structural models corresponding to the monomer of *A. ceylanicum* MIF-2 (Link to the structure 2OS5) [12]. For *Tc*MIF-2, only one possible model was produced, with a C-score of 1.37, a TM value of 0.90 ± 0.06, a RMSD (root-mean-square deviation) of 1.7 ± 1.5 Å, with normalised z-scores less than 4.13. From the best five models obtained for *Hc*MIF-2, the selected model had a C-score of 0.65, a TM value of 0.63 ± 0.14, a RMSD of 6.0 ± 3.7 Å, and normalised z-scores less than 2.51. For *Tc*MIF-2, the catalytic and active site residues that fell within 4 Å of the substrate were Pro-2, Met-3, Lys-33, Pro-34, Glu-63, Ser-64, Ile-65, Leu-102, Val-107 and Val-114 (Figure 3F), whereas the corresponding residues in *Hc*MIF-2 were Pro-2, Met-3, Lys-33, Arg-37, Glu-63, Ser-64, Ile-65, Leu-102, Val-107 and Val-114 (Figure 3G).
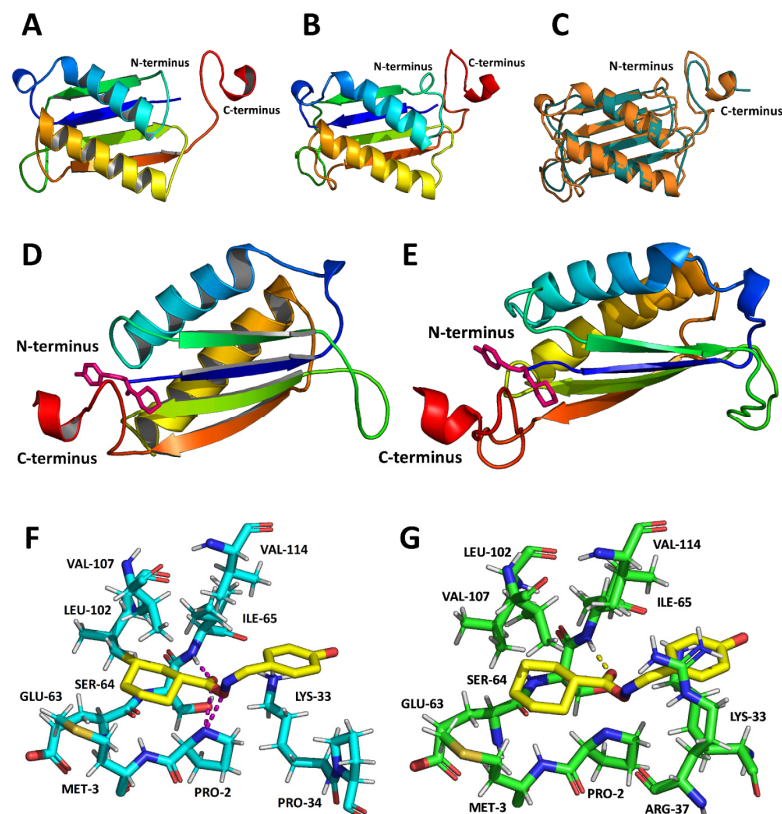

Figure 3. The predicted tertiary structures of the *Tc*MIF-2 and *Hc*MIF-2 monomers. Location of the C- and N-terminus in the predicted tertiary structure of *Tc*MIF-2 (**A**) and *Hc*MIF-2 (**B**). (**C**) Superposition

of the predicted tertiary structure of *Tc*MIF-2 from *T. circumcincta* (blue) and *Hc*MIF-2 from *H. contortus* (orange). Location of the active site (pink) within *Tc*MIF-2 (**D**) and *Hc*MIF-2 (**E**). (**F**) The active site of *Tc*MIF-2 (blue) within 4 Å of the superimposed 2OS5 (yellow) with polar bonds also shown in magenta. (**G**) The active site of *Hc*MIF-2 (green) within 4 Å of the superimposed 2OS5 (yellow) with polar bonds also shown in magenta.

3.3. Recombinant Protein Expression

Maximal production of functional recombinant MIF-2 was obtained in the *E. coli* strain BL21 (DE3) when expression was induced with 0.2% L-arabinose for 4 h at 30 °C. The purified C-terminal His-tagged recombinant *Tc*MIF-2 and *Hc*MIF-2 proteins appeared as single bands of about 16 kDa on SDS-PAGE (Figure 4). The presence of each of the His-tagged recombinant proteins was confirmed by Western blotting.
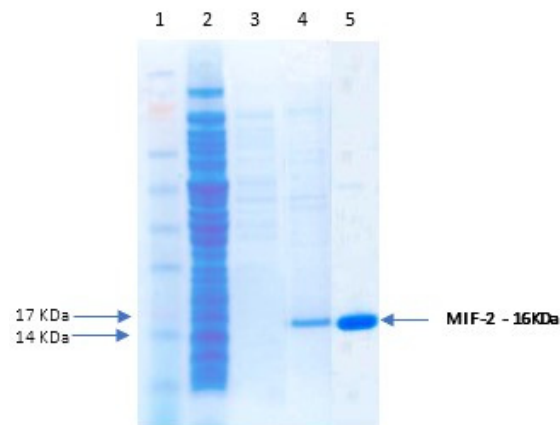
Figure 4. SDS-PAGE of recombinant *Tc*MIF-2 and *Hc*MIF-2. Lane 1- Seeblue Plus2 Pre-stained standard (Invitrogen); lane 2- Unbound material post-passage on column; lane 3- Wash; lane 4- *Tc*MIF-2; lane 5- *Hc*MIF-2.

3.4. Enzyme Assays

The tautomerase activities of *Hc*MIF-2 and *Tc*MIF-2 were similar at 20 nmoles $min^{-1}mg^{-1}$ protein, using 20 μg/mL enzyme in the assay. *Hc*MIF-2 activity was directly proportional to the amount of protein added over the range of 2–20 μg/mL (Figure 5A). The two batches of this purified protein had similar tautomerase activities. Storage at 4 °C, −20 °C or −70 °C reduced activity by approximately 50% (Figure 5B).
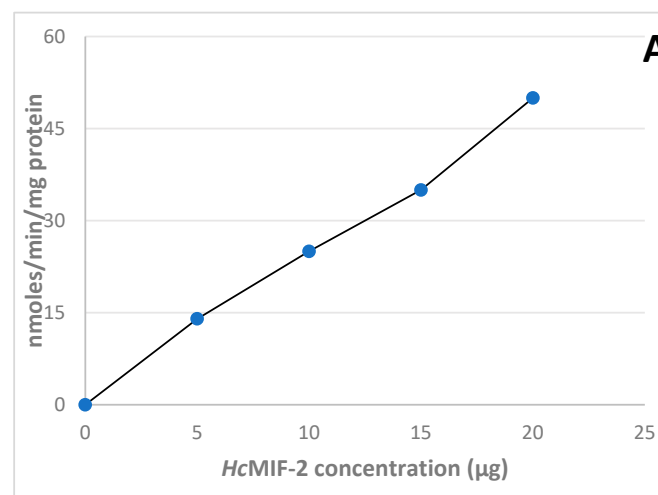

Figure 5. *Cont*.
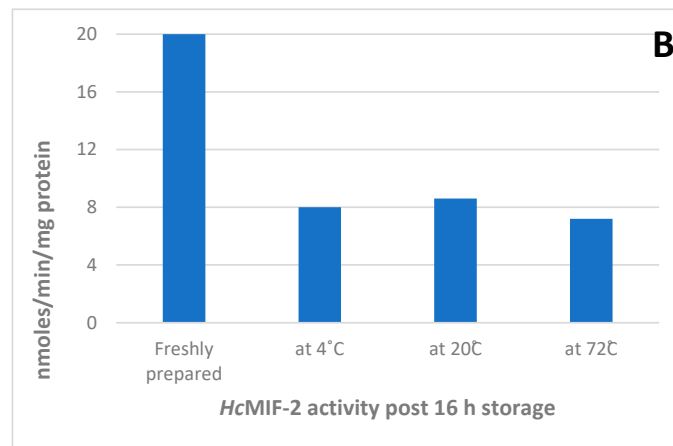
Figure 5. The effect of using increasing concentrations of recombinant *Hc*MIF-2 (**A**) and storage at different temperatures (**B**) on the protein activity (mean ± SD, *n* = 2). The activity was calculated by tautomerisation of the coloured dopachrome methyl ester to its colourless enol form, measured spectrophotometrically at 475 nm.

3.5. Host Recognition

Both *Tc*MIF-2 and *Hc*MIF-2 were recognised in an ELISA by antibodies in both serum and saliva collected from sheep exposed to nematodes in the field (Figure 6). No antibody was detected when serum or saliva samples from parasite-naïve animals was used.
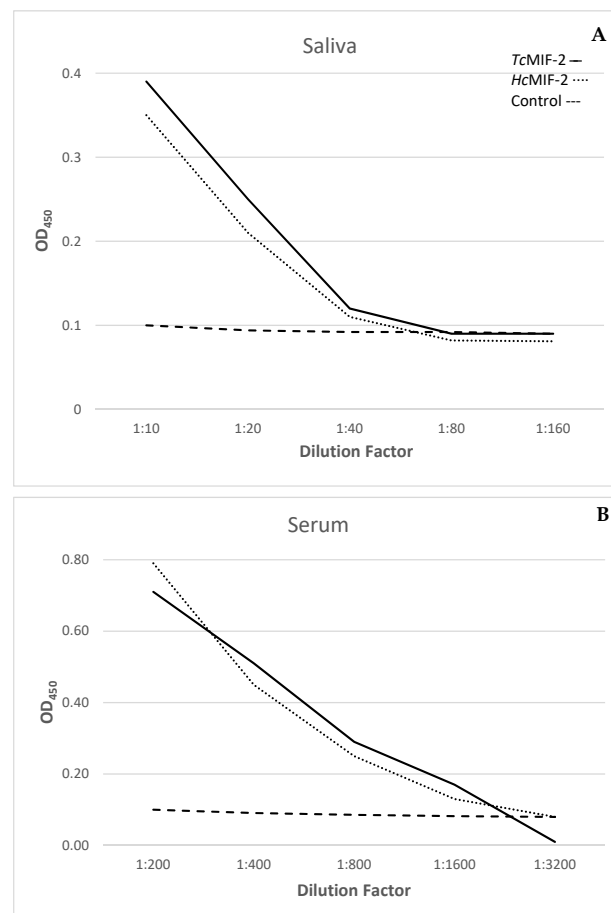
Figure 6. Recognition of *Tc*MIF-2 and *Hc*MIF-2 by serially diluted immune saliva (IgA) (**A**) and serum (IgG) (**B**) but not by parasite-naïve controls.

4. Discussion

This study showed the close structural and functional relationships between recombinant MIF-2 enzymes of the abomasal parasitic nematodes *T. circumcincta* and *H. contortus*. There was also similarity to homologues from several other nematodes. Both proteins were enzymatically typical of MIF-2 characterised from several helminths and were recognised by antibodies in both serum and saliva from field-immune sheep, but not nematode-naïve animals.

T. circumcincta and *H. contortus* MIF-2, designated *Tc*MIF-2 and *Hc*MIF-2, respectively, were shown to be 16 kDa proteins encoded by 342 bp full length cDNA sequences. The amino acid sequence of *Hc*MIF-2 corresponded to the product of the gene designated as HCON_NP_LOC13552, located on chromosome 5 [31], the representative chromosome-level genome of the anthelmintic-susceptible *H. contortus* field strain isolated from pasture-grazed New Zealand sheep.

The two predicted 114 amino acid proteins had 84% homology (Figure 1), were closely related in a phylogenetic tree (Figure 2) and the 3D structures had almost identical active sites (Figures 1 and 3). There was 54–76% homology of *Tc*MIF-2 with MIF-2s of seven nematodes, but it was low with other MIF sequences, including the MIF-2 of the filarial nematodes *B. malayi* and *O. volvulus*. The MIF-2 proteins belonged to a different protein family from MIF-1 of the two nematodes; the MIF-1s were closely related to each other in the phylogenetic tree (Figure 2).

Approximately half of all proteins coded by genes in helminth genomes are currently of unknown function [32]. As a result of the search using PSI-BLAST against the Protein Data Bank (PDB) in this study, a putative function could be assigned to two of the top blast hits currently annotated as hypothetical protein (locus tag EYC32381 to EYC32384 of *A. ceylanicum*) and protein of unknown function (locus tag VDO97074 of *H. polygyrus*), with 65–75% and 80% identity, respectively.

The predicted *Tc*MIF-2 and *Hc*MIF-2 3-dimensional structures and binding and catalytic sites have been determined over a wide range of ligands and shown to be highly conserved (Figure 4). This was also true of many other nematode MIF-2 homologues (Figure 1), with only minor differences in the tautomerase binding site residues.

Given these almost identical active sites, it is unsurprising that the two recombinant enzymes also had quantitatively similar tautomerase activity in the standard assay in which coloured dopachrome methyl ester is changed to its colourless enol form [30]. Given the close similarity of the active sites, it is not surprising that the two recombinant enzymes had similar tautomerase activity in the standard assay in which coloured dopachrome methyl ester is changed to its colourless enol form [30]. Both recombinant *Tc*MIF-2 and *Hc*MIF-2 had similar activities of 20 nmoles min^{-1} mg^{-1} protein, using 20 μg/mL enzyme in the assay. Storage at 4 °C, −20 °C or −70 °C approximately halved tautomerase activity (Figure 5B). It appears that the position of proline at position 2 is cruciasl for tautomerase activity studies [15]. Both recombinant *Tc*MIF-2 and *Hc*MIF-2 have proline at position 2, but the measurable enzymatic activity was many-fold lower when compared with other parasites MIF-2 activity [15,16]. The reason might be the location of the parasite within the host and the % homology of recombinant *Tc*MIF-2 and *Hc*MIF-2 with other MIF-2 proteins. Human filarial parasite *W. bancrofti* was manyfold active, and this might be because of its location within the human lymphatic system. The tautomerase activity of *O. volvulus* might be higher than the recombinant proteins in this study because of significant differences in the amino acid homology, and *O. volvulus* shares only 29% similarity.

Antibodies in both serum and saliva from field-immune, but not nematode-naïve, sheep-recognised recombinant *Tc*MIF-2 and *Hc*MIF-2 in an ELISA (Figure 6). The recognition of both recombinant proteins by antibodies generated by exposure of sheep in the field to native MIF-2s indicates cross-antigenicity of the native and recombinant MIF-2s. This strongly indicates using MIF-2 as a vaccine candidate to control the parasites of ruminants. In addition, the quantitative similarity of recombinant *Tc*MIF-2 and *Hc*MIF-2 in the ELISA suggests that vaccines developed against antigens derived from one of the abomasal parasitic nematodes may also be protective against the other common parasite of sheep.

References

1. Blocki, F.A.; Ellis, L.B.M.; Wackett, L.P. MIF protein are theta-class glutathione S-transferase homologs. *Protein Sci.* **1993**, *2*, 2095–2102. [CrossRef] [PubMed]
2. Leng, L.; Metz, C.N.; Fang, Y.; Xu, J.; Donnelly, S.; Baugh, J.; Delohery, T.; Chen, Y.; Mitchell, R.A.; Bucala, R. MIF signal transduction initiated by binding to CD74. *J. Exp. Med.* **2003**, *197*, 1467–1476. [CrossRef] [PubMed]
3. Bloom, B.R.; Bennett, B. Mechanism of a reaction in vitro associated with delayed-type hypersensitivity. *Science* **1966**, *153*, 80–82. [CrossRef] [PubMed]
4. David, J.R. Delayed hypersensitivity in vitro: Its mediation by cell-free substances formed by lymphoid cell-antigen interaction. *Proc. Natl. Acad. Sci. USA* **1966**, *56*, 72–77. [CrossRef] [PubMed]
5. Salminen, A.; Kaarniranta, K. Control of p53 and NF-κB signaling by WIP1 and MIF: Role in cellular senescence and organismal aging. *Cell. Signal.* **2011**, *23*, 747–752. [CrossRef]
6. Sauler, M.; Bucala, R.; Lee, P.J. Role of macrophage migration inhibitory factor in age-related lung disease. *Amer. J. Physiol.* **2015**, *309*, L1–L10. [CrossRef]
7. Xu, X.; Pang, J.; Chen, Y.; Bucala, R.; Zhang, Y.; Ren, J. Macrophage migration inhibitory factor (MIF) deficiency exacerbates aging-induced cardiac remodeling and dysfunction despite improved inflammation: Role of autophagy regulation. *Sci. Rep.* **2016**, *6*, 22488. [CrossRef]
8. Sparkes, A.; De Baetselier, P.; Roelants, K.; De Trez, C.; Magez, S.; Van Ginderachter, J.A.; Raes, G.; Bucalaf, R.; Stijlemans, B. The non-mammalian MIF superfamily. *Immunobiology* **2017**, *222*, 473–482. [CrossRef]
9. Pastrana, D.V.; Raghavan, N.; Fitzgerald, P.; Eisinger, S.W.; Metz, C.; Bucala, R.; Schleimer, R.P.; Bickel, C.; Scott, A.L. Filarial nematode parasites secrete a homologue of the human cytokine macrophage migration inhibitory factor. *Infect. Immunit.* **1998**, *66*, 5955–5963. [CrossRef]
10. Vermeire, J.J.; Cho, Y.; Lolis, E.; Bucala, R.; Cappello, M. Orthologs of macrophage migration inhibitory factor from parasitic nematodes. *Trend. Parasitol.* **2008**, *24*, 355–363. [CrossRef]
11. Nisbet, A.J.; Bell, N.E.; McNeilly, T.N.; Knox, D.P.; Maizels, R.M.; Meikle, L.I.; Wildblood, L.A.; Matthews, J.B. A macrophage migration inhibitory factor-like tautomerase from *Teladorsagia circumcincta* (Nematoda: Strongylida). *Parasite Immunol.* **2010**, *32*, 503–511. [CrossRef] [PubMed]
12. Cho, Y.; Jones, B.F.; Vermeire, J.J.; Leng, L.; DiFedele, L.; Harrison, L.M.; Xiong, H.; Kwong, Y.K.; Chen, Y.; Bucala, R.; et al. Structural and functional characterisation of a secreted hookworm Macrophage Migration Inhibitory Factor (MIF) that interacts with the human MIF receptor CD74. *J. Biol. Chem.* **2007**, *282*, 23447–23456. [CrossRef] [PubMed]
13. Sharma, R.; Hoti, S.L.; Meena, R.L.; Vasuki, V.; Sankari, T.; Kaliraj, P. Molecular and functional characterisation of macrophage migration inhibitory factor (MIF) homolog of human from lymphatic filarial parasite *Wuchereria bancrofti*. *Parasitol. Res.* **2012**, *111*, 2035–2047. [CrossRef] [PubMed]
14. Younis, A.E.; Soblik, H.; Ajonina-Ekoti, I.; Erttmann, K.D.; Luersen, K.; Liebau, E.; Brattig, N.W. Characterisation of a secreted macrophage migration inhibitory factor homologue of the parasitic nematode *Strongyloides* acting at the parasite-host cell interface. *Microbes Infect.* **2012**, *14*, 279–289. [CrossRef] [PubMed]
15. Ajonina-Ekoti, I.; Kurosinski, M.A.; Younis, A.E.; Ndjonka, D.; Tanyi, M.K.; Achukwi, M.; Eisenbarth, A.; Ajonina, C.; Lüersen, K.; Breloer, M.; et al. Comparative analysis of macrophage migration inhibitory factors (MIFs) from the parasitic nematode *Onchocerca volvulus* and the free-living nematode *Caenorhabditis elegans*. *Parasitol. Res.* **2013**, *11*, 3335–3346. [CrossRef] [PubMed]
16. Chauhan, A.; Sharma, R.; Hoti, S.L. Identification and biochemical characterisation of macrophage migration inhibitory factor-2 (MIF-2) homologue of human lymphatic filarial parasite, *Wuchereria bancrofti*. *Act. Tropica* **2015**, *142*, 71–78. [CrossRef] [PubMed]
17. Zang, X.; Taylor, P.; Wang, J.M.; Meyer, D.J.; Scott, A.L.; Walkinshaw, M.D.; Maizels, R.M. Homologues of Human Macrophage Migration Inhibitory Factor from a Parasitic Nematode. *J. Biol. Chem.* **2002**, *277*, 44261–44267. [CrossRef]

18. Maizels, R.M.; Balic, A.; Gomez-Escobar, N.; Nair, M.; Taylor, M.D.; Allen, J.A. Helminth parasites—Masters of regulation. *Immunol. Rev.* **2004**, *201*, 89–116. [CrossRef]

19. Matoušová, P.; Vokrál, I.; Lamka, J.; Skálová, L. The role of xenobiotic metabolising enzymes in anthelmintic deactivation and resistance in helminths. *Trend. Parasitol.* **2016**, *32*, 481–491. [CrossRef]

20. Wang, Y.; Lu, M.; Wang, S.; Ehsan, M.; Yan, R.; Song, X.; Xu, L.; Li, X. Characterisation of a secreted macrophage migration inhibitory factor homologue of the parasitic nematode *Haemonchus contortus* acting at the parasite-host cell interface. *Oncotarget* **2017**, *8*, 40052–40064. [CrossRef]

21. Marson, A.L.; Tarr, E.K.; Scott, A.L. Macrophage migration inhibitory factor (*mif*) transcription is significantly elevated in *Caenorhabditis elegans* dauer larvae. *Gene* **2001**, *278*, 53–62. [CrossRef]

22. Umair, S.; Ria, C.; Knight, J.S.; Bland, R.J.; Simpson, H.V. Sarcosine metabolism in *Haemonchus contortus* and *Teladorsagia circumcincta*. *Exp. Parasitol.* **2013**, *134*, 1–6. [CrossRef]

23. Knight, J.S.; Broadwell, A.H.; Grant, W.N.; Shoemaker, C.B. A strategy for shuffling numerous *Bacillus thuringiensis* crystal protein domains. *J. Econ. Entomol.* **2004**, *9*, 1805–1813. [CrossRef]

24. Altschul, S.F.; Madden, T.L.; Schäffer, A.A.; Zhang, J.; Zhang, Z.; Miller, W.; Lipman, D.J. Gapped BLAST and PSI-BLAST: A new generation of protein database search programs. *Nucleic Acids Res.* **1997**, *25*, 3389–3402. [CrossRef]

25. Yang, J.; Yan, R.; Roy, A.; Xu, D.; Poisson, J.; Zhang, Y. The I-TASSER Suite: Protein structure and function prediction. *Nat. Method.* **2015**, *12*, 7–8. [CrossRef]

26. Laskowski, R.A.; Rullmann, J.A.C.; MacArthur, M.W.; Kaptein, R.; Thornton, J.M. AQUA and PROCHECK-NMR: Programs for checking the quality of protein structures solved by NMR. *J. Biomol. NMR* **2004**, *8*, 477–486. [CrossRef]

27. Wiederstein, M.; Sippl, M.J. ProSA-web: Interactive web service for the recognition of errors in three-dimensional structures of proteins. *Nucleic Acid. Res.* **2007**, *35*, W407–W410. [CrossRef]

28. Schrodinger, L.L.C. The PyMOL Molecular Graphics System. Available online: https://pymol.org/2/ (accessed on 28 March 2022).

29. Love, C.A.; Lilley, P.E.; Dixon, N.E. Stable high-copy-number bacteriophage lambda promoter vectors for overproduction of proteins in *Escherichia coli*. *Gene* **1996**, *176*, 49–53. [CrossRef]

30. Swope, M.; Sun, H.-W.; Blake, P.R.; Lolis, E. Direct link between cytokine activity and a catalytic site for macrophage migration inhibitory factor. *EMBO J.* **1998**, *17*, 3534–3541. [CrossRef]

31. Palevich, N.; Maclean, P.H.; Baten, A.; Scott, R.W.; Leathwick, D.M. The Genome Sequence of the Anthelmintic-Susceptible New Zealand *Haemonchus contortus*. *Genome Biol. Evol.* **2019**, *11*, 1965–1970. [CrossRef]

32. Palevich, N.; Britton, C.; Kamenetzky, L.; Mitreva, M.; de Moraes Mourão, M.; Slatko, B.E. Tackling hypotheticals in helminth genomes. *Trends Parasitol.* **2018**, *34*, 179–183. [CrossRef] [PubMed]